PERGAMON

Vision Research 38 (1998) 3795–3803

Vision Research

Bilateral symmetry embedded in noise is detected accurately only at fixation

Rick Gurnsey [a,*], Andrew M. Herbert [b], Jeremy Kenemy [a]

[a] *Department of Psychology, Concordia University, 7141 Sherbrooke Street West, Montreal, QC H4B 1R6, Canada*
[b] *École D'Optométrie, Université de Montréal, Québec, Canada*

Received 30 July 1997; received in revised form 13 February 1998

Abstract

Bilateral or mirror symmetry is a ubiquitous feature of biological forms that the visual system could exploit for segmenting an object from a cluttered background. If this is so, the visual system may be prepared to detect symmetry at all retinal locations in parallel. Indeed, a biologically plausible model that responds optimally at axes of symmetry is quite easy to construct. Our data show, however, that if such a mechanism exists, it works with high efficiency only at the fovea. The detection of vertical bilateral symmetry embedded in random noise is very poor unless the axis of symmetry is very close to the point of fixation. This leads to the conclusion that symmetry does not play an important role in image segmentation and that it is important to the visual system only after it is fixated. © 1998 Elsevier Science Ltd. All rights reserved.

1. Introduction

Image segmentation based on abrupt discontinuities in luminance, orientation, chromaticity, texture, motion or disparity is thought by many to be logically prior to the identification of objects. Local contrasts of these types are generally thought to be signalled by low-level visual mechanisms that are applied in parallel at all locations in the visual field. Bilateral symmetry might be added to the foregoing list because it is a highly 'non-accidental' image property that can distinguish a region of potential importance from a background of non-symmetrical 'clutter'. Therefore, the visual system may be prepared to detect symmetry at all retinal locations in parallel. On the other hand, because of its very ubiquity, encoding and signalling symmetry in parallel across the visual field might be a disadvantage for the visual system. Responses arising from behaviourally irrelevant sources (e.g. leaves) would continually bombard the visual system, with negative consequences for both predator and prey.

Whether or not it would be desirable to detect symmetry in parallel, it is easy to construct a physiologically plausible symmetry-selective mechanism that can be applied in parallel to all image locations. The mechanism described in Fig. 1 is a modest variant of models that successfully account for the properties of texture segmentation [1–3], subjective contour encoding [4–6] and second order motion [39,7–9]. The model reliably extracts bilateral symmetry embedded in random noise and its performance degrades gracefully when the percentage of matching dots across the axis of symmetry is reduced [10] and as the width of the symmetric region decreases [11]. Mechanisms of the sort shown in Fig. 1 (selective for many different orientations of symmetry axes) could be applied simultaneously to all image locations, as are simple cells in V1, for example [12].

The view of symmetry as a property extracted by low level-visual mechanisms is supported by neuropsychological data [13] and a growing body of psychophysical results which indicate that briefly presented symmetrical clouds of dots are very easily distinguished from random dot patterns of similar size and density [10,14–16]. Many of these psychophysical studies have examined the discriminability of isolated clouds of symmetrical dots from isolated clouds of random dots (Fig. 2b). Under normal viewing conditions, however, symmetrical objects are embedded in non-symmetrical structures and may appear at any position in the retinal image.

* Corresponding author. Tel.: +1 514 8482243; fax: +1 514 8484545; e-mail: gurnsey@vax2.concordia.ca.

PII: S0042-6989(98)00106-0

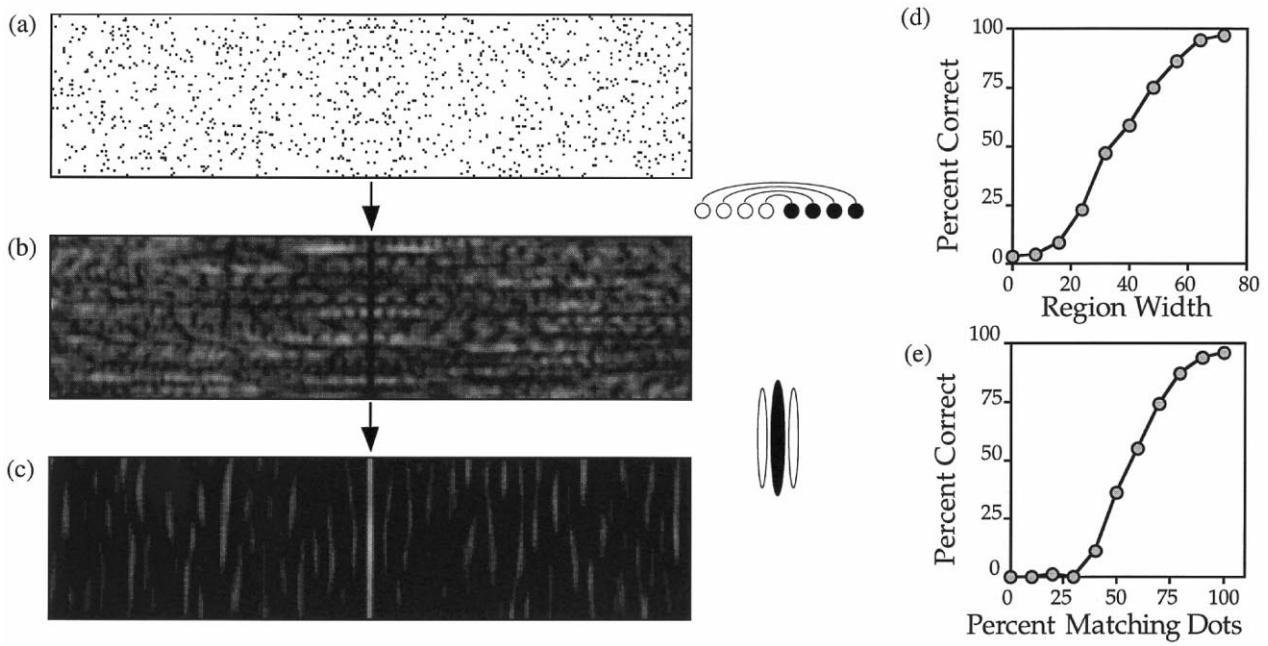

Fig. 1. Panels a,b and c show the transformations of an image that lead to the identification of the axis of symmetry. The pattern in (a) contains a central region of vertically symmetric dots embedded in a much larger region of random dots of equal density. The definition of an image that is symmetric about the y-axis is $I(x, y) - I(-x, y) = 0$ for all x and for $y = 0$. Therefore, one easy way to find symmetry about the y axis is to compute the quantity $d(x, y) = \Sigma_0^n (I(x - n\delta, y) - I(x + n\delta, y))^2$, at each point in the image; for simplicity we refer to this as a dipole computation. The result will be a 'trough' of zero responses along the axis of symmetry (the origin of the coordinate frame can be rotated so that many orientations may be evaluated in parallel). In the present model the image was first low-pass filtered with a small Gaussian kernel prior to the application of the dipole computations. In the present implementation $n = 16$ and $\delta = 2$ pixels. (b) The result of this computation shows a very clear trough which indicates the axis of symmetry. (c) This trough of zero responses can be detected by convolving the representation in (b) with a conventional orientation selective mechanism (shown to the right between panels (b) and (c)). This simple two-stage mechanism has an excellent signal to noise ratio. In images such as (a) the axis of symmetry could be in one of 300 locations and the model detects the axis of symmetry to within two units accuracy 97% of the time simply by locating the maximum response of the second-layer filter. In other words, considered as a 150 alternative forced choice task, the mechanism detects the axis of symmetry 97% of the time. The performance of the model degrades gracefully as the width of the symmetrical region is decreased (d) and as the percentage of matching dots across the axis of symmetry is decreased from 100–0% (e).

These facts must be considered when addressing the question of whether symmetry provides a basis for image segmentation. A task that more closely approximates natural viewing conditions would require the detection of symmetric clouds of dots embedded in a background of random dots (Fig. 1a, 2a) with the location of the symmetric region varied randomly from trial to trial.

In previous studies, when symmetry has been embedded in noise, the axis of symmetry has always been centred at fixation [11,14,17–20]. Conversely, most studies that have manipulated the location of the axis of symmetry have employed isolated symmetry patches [10,16,21–23,38] and the general result has been that performance drops quite modestly as the stimuli are moved from fixation to the periphery. This decline in performance can be slowed, but not eliminated, if the stimuli are increased in size (M-scaled) [24] as eccentricity increases [22]. More recently Tyler and Hardage [23] reported that detection of isolated symmetry could be equated across eccentricities by self-scaling the stimuli; i.e. when the eccentricity of the stimulus presentation doubled, the size of the stimulus is also doubled (scaling of this sort can be accomplished by simply changing the distance from which a stimulus of fixed size is viewed).

Given these observations our empirical questions are (i) how does the detection of embedded symmetry depend on position in the visual field? and (ii) how must such displays be scaled to maintain a constant level of performance at different eccentricities?

2. Method

2.1. Subjects

One female and four male subjects (including two authors, RG and JK) with normal or corrected to normal vision participated in the experiment.

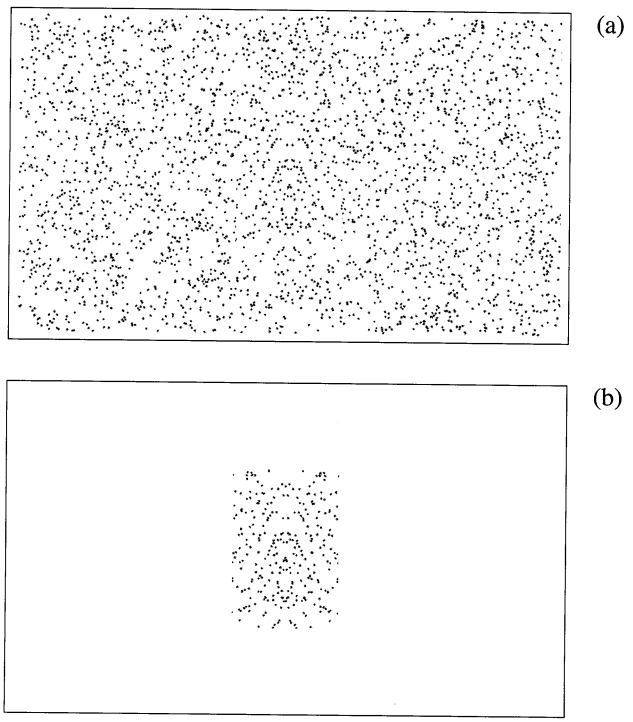

Fig. 2. Exemplars of embedded (a) and isolated (b) symmetry. For illustration, both panels contain exactly the same symmetrical patch (200 × 300 pixels). In (a) this region is embedded in (surrounded by) a much larger region (1024 × 600 pixels) of random dots of the same density.

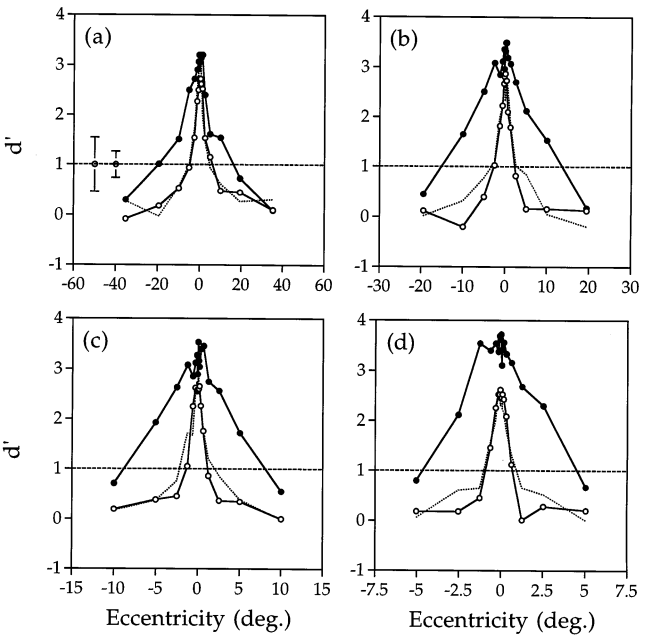

Fig. 3. Average data for five subjects for each viewing distance: (a) 18.75 cm; (b) 37.5 cm; (c) 75 cm; and (d) 150 cm. For the embedded/unblocked condition (no plot symbol) d' was computed from the number of hits at each eccentricity and the average number of false alarms on target absent trials. For the embedded/blocked (unfilled circles) and isolated trials (filled circles), d' was computed from the number of hits and false alarms at each eccentricity. The points with error bars in (a) indicate the largest and average S.E.M. across all eccentricities, viewing distances and conditions.

2.2. Apparatus

Stimuli were presented on a PowerMac 7100/80 computer equipped with a 17 in. colour monitor having a pixel resolution of 1024 horizontal by 768 vertical. Pixel width was approximately 0.29 mm.

2.3. Stimuli

All stimuli were composed of small gaussian blobs that covered 6 × 6 pixels. The blobs were dark grey on a white background (63 cd/m^2) presented at 91% Michelson contrast. Bilaterally symmetric patterns composed of 300 dots were created within a 5.6 cm wide by 8.4 cm high (200 × 300 pixels) window on the monitor[1]. All such patterns were vertically symmetric. The symmetrical patches were either isolated (Fig. 2b) or embedded (Fig. 2a) in a larger background of random dots having the same density. A dark grey fixation spot (four pixels in diameter) was presented at the centre of the screen during the intertrial intervals, and prior to presentation of the patterns.

[1] Jenkins [14] showed that the detection of symmetry asymptotes when the width of a symmetric patch is 1° or greater. Thus, the symmetry patches used in this study were well above any asymptotic width at each distance and eccentricity tested. Dakin and Herbert give a further discussion on the size of the region of integration [20].

2.4. Procedure

Stimuli were presented centred at fixation and at positions ranging from 13.4 cm to the left of fixation to 13.4 cm to the right of fixation ($\pm 13.4/2^n$ for n in [0..7]) for a total of 17 eccentricities. Displays were viewed monocularly at four distances ranging from 18.75 to 150 cm ($150/2^m$ for m in [0..3]) and viewing distance determined the retinal size of the symmetrical region. The patterns were presented under three different conditions. (1) *Isolated.* On each trial, a random or dynamically generated symmetric pattern was presented at one of the 17 eccentricities chosen randomly (Fig. 2b). Each pattern was presented for 75 ms. The task was to determine whether a symmetrical region had been presented or not. Within a block of trials symmetrical patches were presented at each of the 17 eccentricities once along with 17 null trials in which the stimulus contained random dots only. A session consisted of 30 blocks of trials at one of the four viewing distances. (2) *Embedded/unblocked.* The target pattern was presented embedded within random noise (Fig. 2a). Otherwise the parameters were the same as for the isolated condition. (3) *Embedded/blocked.* The target region was placed at only one of two positions symmetrically placed about fixation within a

block of trials so that subjects always knew how far from fixation a symmetrical region might be presented. Separate blocks of trials were run for each of the nine eccentricities at each distance.

3. Results

Fig. 3 presents the average d' results of the five subjects for all three conditions at each of the four distances tested. For the embedded/unblocked condition, d' for detecting symmetry was computed from the number of hits at each of the 17 positions and the mean number of false alarms; false alarm rates could not be associated with a specific screen location given the random presentation of locations within each block. Detection accuracy was very high when the axis of symmetry was centred at fixation and performance dropped precipitously when symmetry was presented away from fixation. This result suggests that when embedded in noise, symmetry detection is very tightly tuned around fixation, leading to the conclusion that bilateral symmetry is unlikely to be an attribute involved in preattentive image segmentation. It could be argued, however, that because the position of the symmetrical region changed randomly from trial to trial, poor performance away from fixation reflects the fact that subjects were operating under a great deal of uncertainty, leading to a strategy that optimised performance around fixation to the detriment of performance at more eccentric positions. For the embedded/blocked condition d' was computed from the number of hits at each eccentricity and the average number of false alarms obtained at the two eccentricities tested within each block. The results show the same very sharp tuning as the embedded/unblocked condition, suggesting that uncertainty about the location of the targets was not a critical determinant of performance. (The tight tuning of embedded symmetry about fixation is consistent with suggestions by Mach [25] and Julesz [26] that vertical bilateral symmetry presented at fixation should be the optimal symmetrical stimulus [16]). The sharp peaks seen in the two embedded conditions contrast with the more gradual drop in performance observed when the symmetric region was isolated in the visual field (Fig. 3a, b, c, d), consistent with previous results [10,16,21,22]. In this case, d' was computed from the number of hits and false alarms at each eccentricity.

Fig. 4 summarizes the pattern of false alarms across screen positions for the three conditions of the experiment. False alarms for the three conditions were calculated for each screen position (distance from fixation in pixels) and then averaged over viewing distance (the manner in which false alarms were computed for each condition is given in the previous paragraph). For the embedded/blocked and isolated conditions false alarm rates are low close to the centre of the screen then increase as the symmetrical patch moves further from fixation. Clearly, subjects have more difficulty with the task at greater eccentricities and tend to relax their response criteria. The false alarm rates for the embedded/blocked and isolated conditions are quite similar in the centre of the display but diverge quickly with eccentricity. Thus, uncertainty increases much more rapidly in the embedded than the isolated case. For the embedded/unblocked condition it was not possible to associate false alarms with different screen positions, so the horizontal line indicates the average false alarm rate over all conditions. The constant level is clearly an over-estimate at fixation and an under-estimate at more eccentric positions. The effect of this under-estimate can be seen in Fig. 3 where in some cases d' in the embedded/unblocked condition exceeds d' in the embedded/blocked condition in the periphery. However, this effect is relatively minor.

Performance in visual detection and discrimination tasks can often be equated across the visual field by scaling or magnifying stimuli [27] at each eccentricity (E) by a factor

$$[F = 1 + E/E_2] \quad (1)$$

The constant E_2 indicates the eccentricity at which the size of a stimulus must be doubled, relative to a foveal standard, to achieve equivalent performance. E_2 is often task specific; an E_2 of about 3 equates the detectability

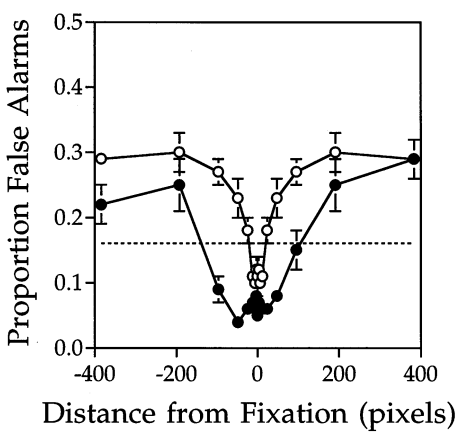

Fig. 4. A summary of the patterns of false alarms in the isolated (filled circles), embedded/blocked (unfilled circles) and embedded/unblocked (no symbol) conditions of the experiment. False alarm rates were calculated for each screen position and averaged over viewing distance; i.e. position is expressed as distance from fixation in pixels. For the embedded/unblocked condition false alarms were computed from the average number of false alarms on all target absent trials. For the embedded/blocked condition false alarms were averaged over all null trials within a block (associated with the two target locations within a block). For the isolated trials, false alarms were computed at each distance from fixation. Error bars (± 1 S.E.M.) reflect the variability in the mean performance at each display position across viewing distances.

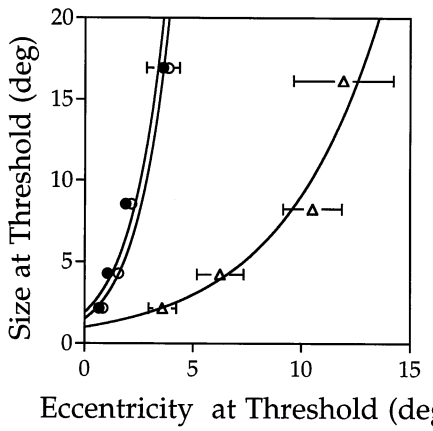

Fig. 5. A plot of eccentricity by symmetric-region size at threshold (d' of 1). The average results of five subjects are shown for the embedded/unblocked (unfilled circles), embedded/blocked and isolated (triangles) conditions. Exponential functions having the form size $= \alpha 10^{(\beta \text{ eccentricity})}$, accounted for 91–97% of the variability in the functions.

of gratings across the visual field and an E_2 of about 0.77 equates performance in certain hyperacuity tasks [27,28]. The E_2 required to equate performance in a given task is often taken to reflect changes in sampling density across the visual field associated with a particular brain area. For example, $E_2 \approx 3$ corresponds approximately to changes in cone sampling at different eccentricities and $E_2 = 0.77$ to the inverse cortical magnification factor [27].

To characterize the magnification required to maintain a constant level of performance at each eccentricity logistic functions were fit to the accuracy data of individual subjects to determine threshold eccentricity (d' of 1) for each viewing distance, or equivalently, for each symmetric region size. On average the fits accounted for 92% of the variability in the scores. Fig. 5 plots eccentricity by symmetric-region width at threshold for the averaged results in each of the three conditions (thresholds have been averaged across the left and right visual fields). Exponential functions (size $= \alpha 10^{(\beta \text{ eccentricity})}$) fit to these data accounted for 91–97% of the variability in the three curves. The (α, β, r^2) triplets for the isolated, embedded/blocked and embedded/unblocked conditions were (0.975, 0.097, 0.968) (1.486, 0.290, 0.936) and (1.881, 0.282, 0.91), respectively.

The calculation of E_2 requires a measurement of size at threshold in a foveal condition. Size thresholds at other eccentricities can be expressed relative to this foveal threshold and it is then simply a matter of finding the parameterization of Eq. (1) (i.e. finding E_2) that best fits these relative size thresholds. Because the present results did not provide a measure of the foveal size thresholds, E_2 can not be calculated in the normal way. However, the data do permit us to put some bounds on what E_2 might be in the conditions studied by making an assumption about what the foveal threshold might be. E_2's based on the means of the three conditions were computed under the assumption that threshold size at fixation is that given by the α value of the best fitting exponential function (see Fig. 5). For the embedded/unblocked, embedded/blocked and isolated conditions, E_2*'s* of 0.46, 0.48 and 1.22, respectively were obtained. When substituted into Eq. (1), these E_2's accounted for 97, 93 and 73% of the variability in the group means, respectively. The estimated E_2's for the two embedded conditions are clearly in the hyperacuity range and that for isolated condition borders on it [28]. Furthermore, to the extent that the assumed foveal size thresholds over-estimate the true threshold sizes, then the resulting E_2's are also over-estimates. That is, if the foveal size thresholds were found to be smaller than those predicted by the exponential functions, then the resulting E_2's would also be smaller. These E_2 calculations must be viewed with some skepticism, however, because the curves in Fig. 5 cannot be linear. When the data in Fig. 5 are fit with linear functions the y-intercepts are all less than 0. Such fits are uninterpretable given that y-intercepts reflect threshold stimulus size for foveal presentations.

4. General discussion

The results show that symmetry is highly salient when presented at fixation[2], irrespective of context (Fig. 3). Over the range of viewing distances examined here (representing an 8-fold change in magnification) performance in the embedded symmetry conditions dropped from extreme sensitivity (mean $d' = 2.9$) to threshold ($d' = 1$) with small shifts away from fixation. Thus, even when the display subtended 16°, performance fell to threshold within 3.6–3.85° of fixation. Therefore, if the high sensitivity at fixation in the embedded conditions results from a mechanism such as that described in Fig. 1, that mechanism works with high efficiency only at fixation.

There are three features of the present data that need an explanation; (i) the sensitivity loss with eccentricity

[2] In this experiment it is unclear whether the proximity of symmetry to fixation or to the vertical meridian is most important for the salience of symmetry because patterns were only presented to the left and right of fixation. Two studies are consistent with the idea that the location of symmetry relative to fixation, not the vertical midline, determines the salience of symmetry. First, Wenderoth [19] showed symmetry was more easily detected in uniformly symmetric regions than for symmetric annuli, where the symmetric axis was aligned with the vertical meridian but random elements were presented at fixation. Second, Herbert et al. [38] showed that the detectability of symmetry falls off for isolated symmetric regions centred at different positions along the horizontal or vertical midlines.

in the isolated condition; (ii) the much quicker sensitivity loss with eccentricity in the embedded conditions and; (iii) the fact that blocking in the embedded condition has no effect.

We assume that symmetry is detected through a multi-scale version of the model depicted in Fig. 1. Both larger- and smaller-scale versions of the mechanism are applied to the image in parallel and their responses combined at each retinal position. We also assume that internal noise of equal magnitude is added to the response of the multi-scale symmetry selective mechanisms at each eccentricity. Signals (symmetrical patches) and noise (random dots) elicit different response distributions from the multi-scale mechanism. On a given trial the subject must determine whether a particular response of the mechanism comes from the signal or noise distribution. The subject determines a criterion response that the symmetry-selective mechanism must exceed before the presence of symmetry is reported. The d' values that result from the pattern of hits and false alarms reflects the separation between the two distributions.

In the isolated condition subjects are able to develop a model of the signal and noise distributions at each eccentricity and set their criteria accordingly; i.e. different response criteria are set at each eccentricity. As stimuli are moved into the periphery high frequencies are attenuated by reduced sampling and greater convergence in the retina. As a result, the total stimulus energy transferred through the visual system decreases with eccentricity, as does the amplitude of the symmetry-selective mechanism's response to both signal and noise. Without internal noise, the change in amplitude would not necessarily change the number of standard units separating the distributions (i.e. d') at each eccentricity. The addition of internal noise, however, will reduce the separation between the signal and noise distributions in both conditions. However, the internal noise will have a greater effect in the low amplitude (eccentric) conditions than in the high amplitude (foveal) conditions. Therefore, sensitivity declines with eccentricity in the isolated condition because a loss of stimulus energy permits internal noise to mask any difference in the mechanism's response to signal and noise.

The two embedded conditions elicited similar sensitivities at each eccentricity. Therefore, knowing the location of the embedded region did not influence sensitivity. A locally acting symmetry-selective mechanism should not be affected by the noise which surrounds the symmetrical region in the embedded cases, so we would expect the signal and noise distributions at each eccentricity in the embedded conditions to be the same as in the isolated conditions. The equivalence of sensitivity of the embedded/blocked and embedded/unblocked conditions demonstrates that subjects are not able to form a decision criterion for each eccentricity as they were able to do in the isolated condition.

We suggest that the d' difference between the isolated and embedded cases in the periphery results from a change in the noise distribution against which the signal is compared. In the isolated case the relevant noise distribution was specific to the eccentricity at which signal and noise were presented. In the embedded case, however, it is possible that the response criterion at every eccentricity is determined by the symmetry-selective mechanism's response to noise at fixation. In other words, subjects are not able to ignore the symmetry-selective mechanism's response to noise at fixation in the embedded conditions. Consequently, performance in the embedded conditions should decrease very quickly with eccentricity. As the eccentricity at which the symmetrical patch is presented increases, it becomes less likely that a response to this signal will exceed a criterion that is determined by the mechanism's response to noise at fixation.

One cannot discount the possibility that the loss of the symmetrical outlines [10,19] in the embedded conditions contributed to the relatively greater sensitivity losses observed at greater eccentricities. On the other hand, because of the density of dots used in the stimuli, the borders of the random and symmetric patterns in the isolated conditions (see Fig. 2b) are both rectangular in the low frequency channels available in the periphery. This similarity in shape might be expected to increase the similarity between the symmetrical and noise regions rather than providing a basis for discrimination. Another possibility is that the horizontal and vertical edges defining the rectangular aperture in which the isolated symmetrical patches were presented somehow aided the detection of the axis of symmetry. Again, this possibility cannot be ruled out. Regardless of the source of the 'isolated advantage', the main point is that symmetry is poorly detected in noise if not presented very close to fixation and therefore symmetry is unlikely to make a substantial contribution to image segmentation on it own.

The ease with which isolated displays can be identified as symmetric or not [10,16,21,22] may give a misleading impression of how salient symmetry is in general. We originally asked whether symmetry could be used to segment images prior to object identification. The fact that detection of embedded symmetry is so tightly tuned around fixation suggests that it is not a property that contributes significantly to image segmentation. Rather, once a region has been fixated for some other reason its symmetry becomes a highly salient property. This conclusion is complimentary to that of Labonté et al. [17]. In their study, the two halves of a symmetrical stimulus were presented at increasing distances from fixation. The symmetrical halves were composed of either oblique or vertical line segments which

were always embedded in a background of randomly placed vertical lines. At fixation the two element types produced indistinguishable performance (under both conditions performance was on the ceiling). When the two halves were separated by 6.6°, symmetry was more easily seen for patches comprising oblique line segments than for patches of vertical line segments. In other words, when the elements of the symmetrical halves were distinguished from the background texture by an orientation difference their symmetry was more easily discerned than when no such segmentation was possible. The Labonté et al. results would imply that our embedded and isolated conditions could be equated if an additional difference (e.g. a wavelength difference) between the symmetrical region and background noise was added. This remains an empirical question.

It is worth noting that Labonté et al. [17] addressed the unusual case of two halves of a symmetrical pair separated by a large distance rather than the more naturalistic conditions described here. Their stimuli would defeat a locally acting mechanism such as described in Fig. 1 [29]. Our data show what theirs did not, namely, that local symmetrical structure is poorly detected in noise away from fixation. In comparing the present results with those of Labonté et al. it should be kept in mind that their stimuli were presented for durations 20 times longer than ours.

Saarinen [22] found that magnifying isolated symmetric displays according to the equation of Rovamo and Virsu [24] ($F = \alpha\ (1 + E/3 + \varepsilon\ E^3)$, where $\alpha = 7.99$ and $\varepsilon\ = 0.00007$) failed to equate performance at all eccentricities. In recent years it has become evident that the magnification function required to equate performance across eccentricities is task dependent [30–32]. Therefore, it is likely that the scaling required to equate symmetry detection across the visual field is not the same as that required to equate grating detection. This interpretation is consistent with the earlier E_2 analysis of the isolated condition. On the other hand, as discussed earlier, the scaling that equates performance at each eccentricity is non-linear (Fig. 5); i.e. the data do not conform to the simple linear scaling strategy described by Eq. (1). Further research required here as well to determine the range of conditions under which this non-linear scaling function obtains.

Tyler and Hardage [23] examined the detection of isolated symmetry at a range of eccentricities using stimuli related to those of Labonté et al. [17]. In one of their conditions two sectors of fixed size, both of which were symmetric across the vertical midline, were placed above and below fixation. Detection accuracy was measured as a function of presentation duration for several viewing distances. Stimuli were 'self-scaled' (as they were in the present experiment) so that the size of the stimulus doubled as viewing distance was halved. They found that sensitivity (the reciprocal of the exposure duration yielding $d' = 0.5$) was constant at all viewing distances that placed the symmetrical region at least 2° from fixation. In other words, when the size and eccentricity of the stimulus was doubled (by halving the viewing distance) sensitivity remained constant. Self-scaling would predict that doubling the stimulus size would double threshold eccentricity. However, this result was not generally found in the present experiment. The average eccentricity increments with size doubling for the embedded/unblocked, embedded/blocked and isolated conditions were 1.76, 1.64 and 1.40, respectively. That is, doubling stimulus size moved threshold eccentricity less than a factor of two further into the periphery. The isolated condition most closely matches the conditions of Tyler and Hardage's experiment and yet produces the most divergent results. This discrepancy is probably due to methodological differences. Tyler and Hardage tested only one stimulus size at each eccentricity. If all stimuli exceeded the resolving limits of the visual system then there would be no reason to expect different exposure duration thresholds at each eccentricity. In the present experiment stimuli of many sizes were tested at many eccentricities to determine the eccentricity dependent limitations on sensitivity.

Although symmetry detection has been studied intensely over the years, very few neural models of the process have appeared in the literature. Those that have appeared are quite different in form. Dakin and Watt [29,33] presented a model which exploits the fact that, across an axis of symmetry, there will be a preponderance of dipoles perpendicular to the axis of symmetry [14]. Their model encodes 'zero-bounded region blobs' using Watt's [34] image description representation. When an axis of symmetry is present, the centroids of parallel, elongated blobs (perpendicular to the axis of symmetry) will be collinear. Dakin and Watt showed that this symmetry detection strategy could successfully explain characteristics of symmetry detection observed in several classic studies [10,11]. The computation of the centroids of zero-bounded blobs might be accomplished by double end-stopped cells known to abound in the visual cortex. Replacing the dipole computations in Fig. 1 with double end-stopped mechanisms [6] would yield a biologically plausible alternative to the dipole computations shown in Fig. 1. Such a model would also represent a variant of the Dakin and Watt model that is more directly connected to known physiological structures in the visual system.

Wilson and Wilkinson [35] constructed 'radial frequency patterns' by modulating the radii of circular patterns by the sum of two cosines having different radial frequencies. The degree to which the resulting pattern were symmetrical was determined by the rela-

tive phases of the cosine modulations. Subjects were very sensitive to deviations from symmetry. Wilson and Wilkinson modelled these results using non-Cartesian basis functions [36,37]. The architecture of their model is quite different from the dipole model and that of Dakin and Watt, and it is not yet clear which of these three proposals provides a more comprehensive account of existing data.

5. Conclusion

Symmetry is unlikely to play an important role in preattentive image segmentation because it is so poorly discriminated when embedded in noise. The extremely high foveal sensitivity to symmetry in noise has to be reconciled with the rapid deterioration in performance when the symmetric region is moved away from fixation. Perhaps there are simply too many behaviourally irrelevant sources of symmetry in the world, so the visual system avoids being drawn to symmetrical regions in the periphery. However, once a particular image location is fixated, symmetry in this region becomes highly salient.

Acknowledgements

This research was supported by NSERC and FCAR Research Grants to Rick Gurnsey. We thank Frédéric Poirier, Michael von Grünau and David Fleet for their comments, and Peter April for excellent programming support.

References

[1] Rubenstein BS, Sagi D. Spatial variability as a limiting factor in texture-discrimination tasks: implications for performance asymmetries. J Opt Soc Am A 1990;7:1632–43.
[2] Landy MS, Bergen JR. Texture segregation and orientation gradient. Vis Res 1991;31:679–91.
[3] Gurnsey R, Pearson P, Day D. Texture discrimination along the horizontal meridian: effects of magnification, frequency content and micropattern orientation. J Exp Psychol: Hum Percept Perform 1996;22:738–57.
[4] Gurnsey R, Humphrey GK, Kapitan P. Parallel discrimination of subjective contours defined by offset gratings. Percept Psychophys 1992;52:263–76.
[5] Wilson HR, Richards WA. Curvature and separation discrimination at texture boundaries. J Opt Soc Am A 1992;9:1653–62.
[6] Gurnsey R, von Grünau M. Illusory contour-motion arising from translating terminators. Vis Res 1997;37:1007–24.
[7] Chubb C, Sperling G. Drift-balanced random stimuli: a general basis for studying non-Fourier motion perception. J Opt Soc Am A 1988;5:1986–2007.
[8] Fleet DJ, Langley K. Computational analysis of non-Fourier motion. Vis Res 1994;34:3057–79.
[9] Gurnsey R, Fleet D, Potechin C. Second order motions contribute to vection. Vis Res 1998;38:2801–16.
[10] Barlow HB, Reeves BC. The versatility and absolute efficiency of detecting mirror symmetry in random dot displays. Vis Res 1979;19:783–93.
[11] Jenkins B. Component processes in the perception of bilaterally symmetric dot textures. Percept Psychophys 1983;34:433–40.
[12] Hubel DH, Weisel TN. Receptive fields, binocular interaction and functional architecture in the cat's visual cortex. J Physiol Lond 1962;160:106–54.
[13] Driver J, Baylis GC, Rafal R. Preserved figure-ground segregation and symmetry detection in visual neglect. Nature 1992;360:73–5.
[14] Jenkins B. Redundancy in the perception of bilateral symmetry in dot textures. Percept Psychophys 1982;32:171–7.
[15] Wenderoth P. The salience of vertical symmetry. Perception 1994;23:221–36.
[16] Herbert AM, Humphrey GK. Bilateral symmetry detection: testing a 'callosal' hypothesis. Perception 1996;25:463–80.
[17] Labonté F, Shapira Y, Cohen P, Faubert J. A model for global symmetry detection in dense images. Spat Vis 1995;9:33–55.
[18] Tyler CW, Hardage L, Miller RT. Multiple mechanisms for the detection of mirror symmetry. Spat Vis 1995;9:79–100.
[19] Wenderoth P. The role of pattern outline in bilateral symmetry detection with briefly flashed dot patterns. Spat Vis 1995;9:57–77.
[20] Dakin SC, Herbert AM. The spatial region of integration for visual symmetry detection. Proc R Soc Lond Series B, (In Press).
[21] Masame K. Detection of symmetry in complex patterns: does symmetrical projection to the visual system necessary for the perception of symmetry? Tohoku Psychol Folia 1983;42:27–33.
[22] Saarinen J. Detection of mirror symmetry in random dot patterns at different eccentricities. Vis Res 1988;28:755–9.
[23] Tyler CW, Hardage L. In: Tyler CW, editor. Human Symmetry Perception. Utrecht, Netherlands: VSP, 1996:157–71.
[24] Rovamo J, Virsu V. An estimation and application of the human cortical magnification factor. Exp Brain Res 1979;37:495–510.
[25] Mach E. Contributions to the Analysis of the Sensations. La Salle, IL: Open Court, 1897 CM Williams, Translator.
[26] Julesz B. Foundations of Cyclopean Perception. Chicago, IL: University of Chicago Press, 1971.
[27] Levi DM, Klein SA, Aitsebaomo AP. Vernier acuity, crowding and cortical magnification. Vis Res 1985;25:963–77.
[28] Wilson HR, Levi D, Maffei L, Rovamo J, De Valois R. The perception of form: retina to striate cortex. In: Spillman L, Werner JS, editors. Visual Perception: The Neurophysiological Foundations. New York: Academic Press, 1990:231–72.
[29] Dakin SC, Watt RJ. Detection of bilateral symmetry using spatial filters. Spat Vis 1994;8:393–413.
[30] Whitaker D, Rovamo J, McVeigh D, Mäkelä P. Spatial scaling of vernier acuity tasks. Vis Res 1992;32:1481–91.
[31] Whitaker D, Mäkelä P, Rovamo J, Latham K. The influence of eccentricity on position and movement acuities as revealed by spatial scaling. Vis Res 1992;32:1913–30.
[32] Whitaker D, Latham K, Mäkelä P, Rovamo J. Detection and discrimination of curvature in foveal and peripheral vision. Vis Res 1993;33:2215–24.
[33] Dakin SC, Hess R. The spatial mechanisms mediating symmetry perception. Vis Res 1997;37:2915–30.

[34] Watt R. Understanding Vision. London: Academic Press, 1991.
[35] Wilson HR, Wilkinson F. Symmetry thresholds for radial frequency petterns. Bilateral symmetry detection as a function of eccentricity. Invest Opthalmol Vis Sci 1997;38(4):1188.
[36] Caelli T, Dodwell PC. Orientation-position coding and invariance characteristics of pattern discrimination. Percept Psychophys 1984;36:159–68.
[37] Gallant JL, Braun J, van Essen DC. Selectivity for polar, hyperbolic, and cartesian gratings in macaque visual cortex. Science 1993;259:100–3.
[38] Herbert AM, Faubert J, Humphrey GK. Bilateral symmetry detection as a function of eccentricity. Invest Ophthalmol Vis Sci 1997;38(4):638.
[39] Wilson HR, Mast R. Illusory motion of texture boundaries. Vis Res 1993;33:1437–46.